Hindawi
Advances in Materials Science and Engineering
Volume 2022, Article ID 5942506, 7 pages
https://doi.org/10.1155/2022/5942506

Research Article

Material Behaviour of Three Blade Propeller Using Metal Additive Manufacturing Techniques

Avinash Malladi,[1] K. Karunakaran,[1] R. Saravanan,[2] and Yalew Asres[3]

[1]*Department of Mechanical Engineering, School of Engineering, Vels Institute of Science Technology and Advanced Studies, Chennai, Tamil Nadu, India*
[2]*Institute of Mechanical Engineering, Saveetha School of Engineering, Saveetha Institute of Medical and Technical Sciences (SIMATS), Saveetha University, Chennai 602105, Tamil Nadu, India*
[3]*Department of Mechanical Engineering, Faculty of Manufacturing Institute of Technology, Hawassa University, Ethiopia*

Correspondence should be addressed to K. Karunakaran; ksivasakthi1966@gmail.com and Yalew Asres; yalewa@hu.edu.et

Received 6 May 2022; Revised 15 July 2022; Accepted 22 July 2022; Published 15 September 2022

Academic Editor: Alicia E. Ares

The defects stored during the fusion of the laser with the metal powder bed determine the optimal performance of fatigue and lifelong disintegration of the formed metal components. The advantage of using recent technologies of prototyping is very much powerful in understanding the physical process. The current works provide the details of the same for a 3-blade propeller with its thermomechanical approach to identified parameters. The results provide the materials used and their behaviour with the parameters which conclude in prescribing the material for the various applications. The investigation aimed to optimize the position of the object (3-blade Propeller) and material for printing through simulation before it was printed. The material choices of aluminium AlSi10 Mg, stainless steel 17–4 and stainless steel 316L were considered. The ten different object positions were considered and ranked by the minimum support area required. The top and bottom-ranked positions were further investigated with three different materials, namely Aluminium AlSi10 Mg, atainless steel 17–4, and stainless steel 316L, in which the Rank 1 position, the material of Aluminium AlSi10 Mg exhibits the minimum of maximum displacement (2.348e-01 mm), plastic strain (0.05), and the Von Mises Stress (2.086e+02 MPa).

1. Introduction

3D-printing technology has resolved many manufacturing challenges and some of the novel and notable contributions are presented here. Reference [1] adopted the powder bed fusion method to prepare the implant and avoided implant and natural bone modulus mismatch with Beta-titanium alloys. Reference [2] experimented with the influence of Zirconium reinforcement aluminium alloy (AA) 7075 in producing crack-free components in the laser powder bed fusion method. The results reveal that the increased quantity of reinforcement decreased the crack density. Reference [3] highlighted that the most influencing process parameters are hatch distance, laser power, and scan speed in laser powder bed fusion technique, and investigated the influence of part geometry on defect and developed a geometric-based defect model and a semianalytical thermal model to locate the region in which the solidification will take place well and the same was validated by producing a specimen with AISI 316L Stainless steel. Reference [4] addressed the inconsistency in manufacturing products with laser powder bed fusion with machine learning at preprocessing like designing, then used the same for control then it integrated to postprocessing. The spheroidization system (TekSphero-15) was employed in laser powder bed fusion to improve the ductility and lower the tensile strength of AISI 304L stainless steel parts [5]. A machine learning model introduced for linking of process-structure-property in two different 3D printing techniques like electron beam powder bed fusion and laser powder bed fusion through machining behaviour and validated it with

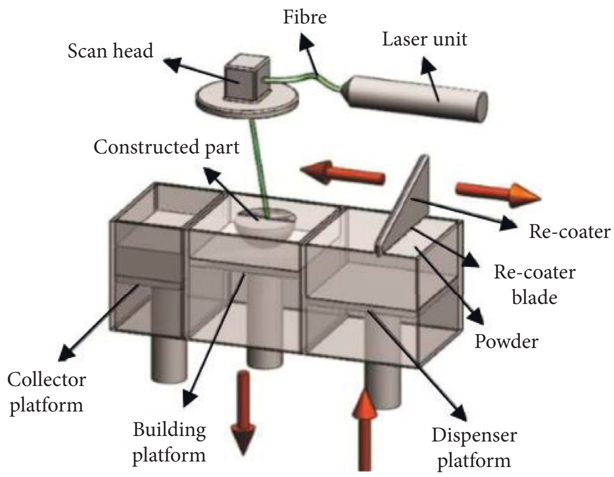

Figure 1: Schematic representation of DMLS Process.

fabricating samples of heterogeneous material of Ti–6Al–4V AM. It was ensured that corrosion resistance, fatigue behaviour, and machining behaviour could be achieved [6]. Machine learning technological support was added by building a model for linking the process-structure property to print the part with overhanging features in a laser powder bed fusion technique. The Ti–6Al–4V samples were produced and validated [7]. A lattice support structure (thermally conductive) was introduced in which a transient analysis model was combined with the equivalent static loads method with lattice structure topology optimization. This proposed system reduced the overall computational cost significantly [8]. Three-blade propeller models used in aerospace are more in demand for studying the structure and behaviour of the materials in applications [9]. Choosing the right number of propeller blades depends on several parameters, including a given jet engine power, operating RPM propeller, scope limits, and operating requirements [10–15]. If these features are regularly maintained, the efficiency of the propeller will decrease as additional blades are added [16]. However, as engine power grows, more blades are often needed to make better use of increasing power and to produce thrust [17]. Therefore, the most effective number of propeller blades in a plane depends on the combination of these features, which, of course, will vary depending on the aircraft [18].

The metal additive manufacturing process is a unique approach in comparison with traditional manufacturing [19–26]. According to ISO/ASTM terminology, the direct metal laser sintering (DMLS) process is a kind of additive manufacturing method. As it prints by the layers formed by powders and heated for bonding subsequently, it is under the class of powder bed fusion. The schematic representation of the DMLS process is depicted in Figure 1. The DMLS was especially developed for printing metal alloy products. In view of its unique advantages, this investigation considered the printing of 3-blade metallic propeller. This study process involved designing and simulating the process by considering three different materials and 10 different positions of the propeller.

2. Process Flow in DMLS

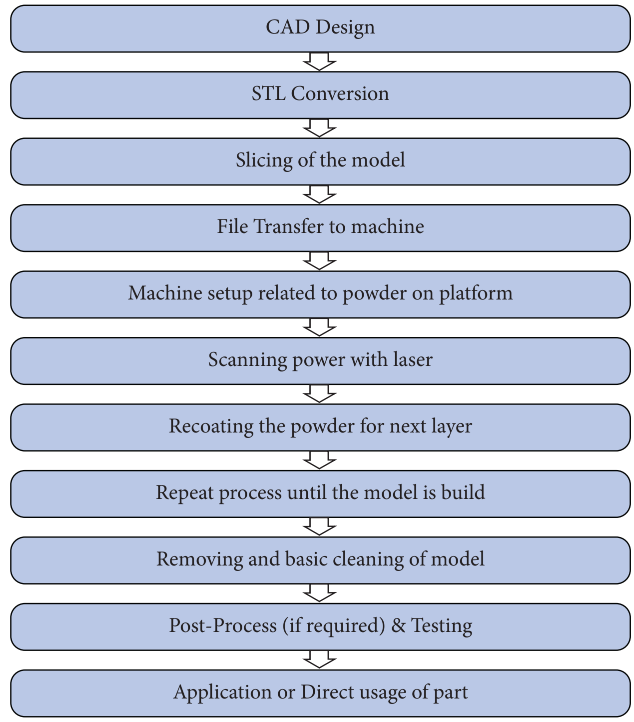

3. Designing

Figure 2 shows that the 3-blade propeller has been designed by Autodesk inventor as it has the flexibilities in designing complex structures [27–34]. The modelling has taken 5 steps in reaching the below-mentioned model:

4. Materials

The materials chosen are based on the research and are also available in the software that has been chosen. For the same we have used the Altair Inspire for undergoing the simulation process, the materials chosen are:

(i) Aluminium AlSi10 Mg
(ii) Stainless Steel 17–4
(iii) Stainless Steel 316L

The above materials listed above are compatible materials for the DMLS process. Hence the details of the material properties which were already defined in the software are presented here for better understanding. The general properties of selected materials are furnished in Table 1 , and 2 shows the thermal properties of materials for the 3-blade propeller, and their mechanical properties are presented in Table 3.

5. Positioning of the Part

As this is the initial process of starting the simulation, the key aspect of this step is to understand and estimate the time and material consumption for making the product [20–23]. The following are the various positions that has been studied

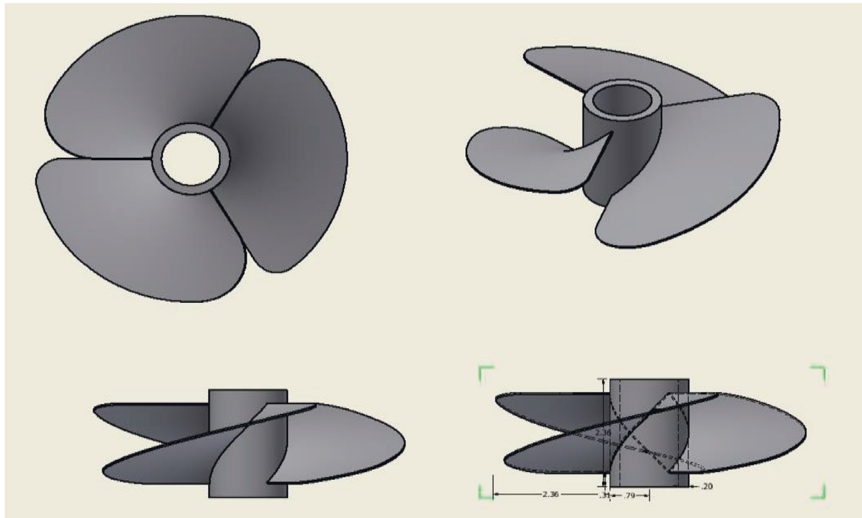

Figure 2: Design of 3-blade propeller.

Table 1: General Properties of materials for 3-blade Propeller.

S. No.	General properties	Aluminium AlSi10 Mg	Stainless steel 17–4	Stainless steel 316L
1	Density	2.67e-06 kg/mm3	7.65e-06 kg/mm3	7.9e-06 kg/mm3
2	Plastic modulus	2.3e+08	2.1e+08	5.14e+08
3	Plastic exponent	0.12	0.3	0.508
4	Emissivity	0.18	0.59	0.9
5	Convection coefficient	12.7	12.7	5

Table 2: Thermal Properties of materials for 3-blade Propeller.

S. No.	Thermal properties	Aluminium AlSi10 Mg	Stainless steel 17–4	Stainless steel 316L
1	Specific heat	915 K	475 K	600 K
2	Conductivity	150 W/mK	13 W/mK	16.2 W/mK
3	Reference temperature	293 K	293 K	293 K
4	Temperature exponent	0.7	1.12	0.533
5	Ambient temperature	293 K	293 K	293 K
6	Melting temperature	853.15 K	1690 K	1723 K

Table 3: Mechanical Properties of materials for 3-blade Propeller.

S. No.	Mechanical properties	Aluminium AlSi10 Mg	Stainless steel 17–4	Stainless steel 316L
1	Young's modulus	7.76e + 10	1.7e + 11	1.515*e* + 11
2	Poisson ratio	0.336	0.306	0.3
3	Yield stress	2.04e + 08	5.4e + 08	5.14*e* + 08
4	Coefficient of thermal expansion	2.1e-05	1.4e-05	1.5*e*-05

Table 4: Variations of physical features are required based on the position to be printed.

Rank	Supported area (cm2)	Support volume (cm2)	Outbox volume (cm2)	Height (mm)	Centre of gravity height (mm)
1	29.900	87.121	1365	141.1	70.7
2	29.212	100.520	1108	150	75
3	29.278	100.808	1122	150	75
4	29.433	101.530	1108	150	75
5	29.846	101.885	1122	150	75
6	30.466	103.793	1108	147.7	72.7
7	32.006	107.250	1108	147.7	75
8	166.747	300.539	1108	50	21.9
9	166.747	300.540	1122	50	21.9
10	166.747	434.134	1108	50	28.1

Table 5: Top- and Bottom-ranked positions of 3-blade propeller.

S.No.	Rank	Image of the position
1.	1	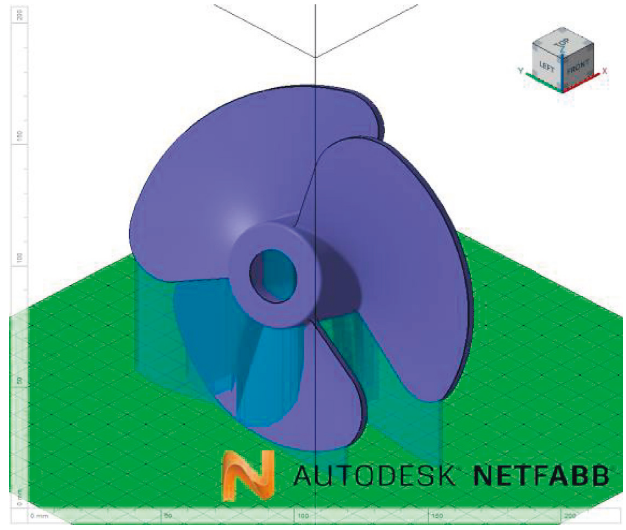
2.	10	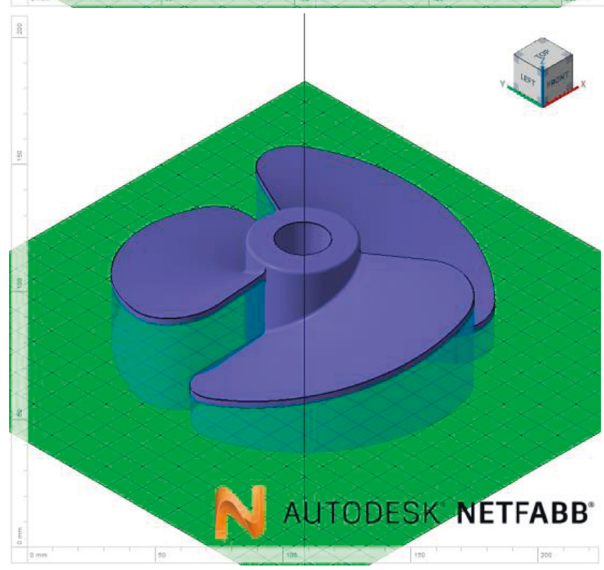

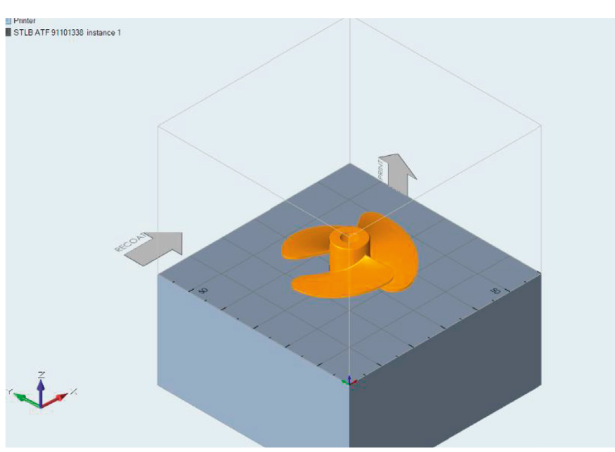

Figure 3: Showing the position of the part which is going to be developed over the metal powder bed and we can see the Direction of Print and Recoat movement.

Table 6: 3D -printing parameters.

S.. No.	Parameters	Values
1	Velocity (mm/s)	1200.00
2	Laser power (W)	600.00
3	Powder layer thickness (mm)	0.03
4	Powder absorption (%)	10.00
5	Cooling time (s)	150.00
6	Base temperature (K)	298.00

Table 7: Simulation results For the Rank 1 position.

S. No.	Results domain	Aluminium AlSi10 Mg		Stainless steel 17–4		Stainless steel 316L	
		Max	Min	Max	Min	Max	Min
1	Displacement (mm)	2.348e-01	0	2.908e-01	0	3.056e-01	0
2	Plastic strain	0.05	0	0.23	0	0.23	0
3	Von mises stress (MPa)	2.086e+02	9.510e-01	2.100e+02	3.413e-01	1.163e+02	1.048
4	Nodal temperature (K)	307.03	306.02	364.89	281.79	358.49	287.74
5	Temperature of metal (K)	3.065e+02	3.065e+02	3.615e+02	3.248e+02	3.584e+02	3.250e+02

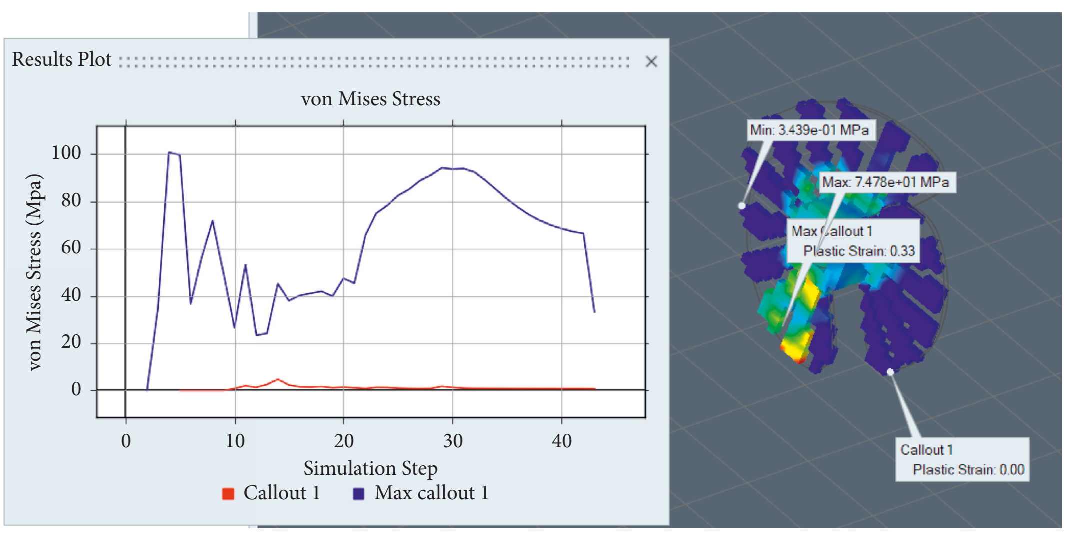

Figure 4: Von mises stress various callout positions and a graph representing the von mises vs simulation step for Rank 1.

Table 8: Simulation results For the Rank 10 position.

S. No.	Results domain	Aluminium AlSi10 Mg		Stainless steel 17–4		Stainless steel 316L	
		Max	Min	Max	Min	Max	Min
1	Displacement (mm)	2.411e-01	0	2.507e-01	0	2.657 e-01	0
2	Plastic strain	0.1	0	0.5	0	0.33	0
3	Von mises stress (MPa)	6.655e+01	2.558e-01	1.455 e + 02	1.984 e-0.3	7.478 e + 01	3.439e-01
4	Nodal temperature (K)	319.44	283.34	795.60	247	784.91	251.46
5	Temperature of metal (K)	3.121e + 02	3.081e + 02	7.956e + 02	3.752e + 02	7.849e + 02	3.715e + 02

in Autodesk Netfabb software with various design aspects: The position varied from vertical to horizontal in about 10 different positions. The obtained results of the variation of physical features required based on the position to be printed are furnished in Table 4. The ranking was done based on the minimum amount of support required to print. The top-ranked (vertical) and bottom-ranked (horizontal) position of the 3-blade propeller were furnished in Table 5.

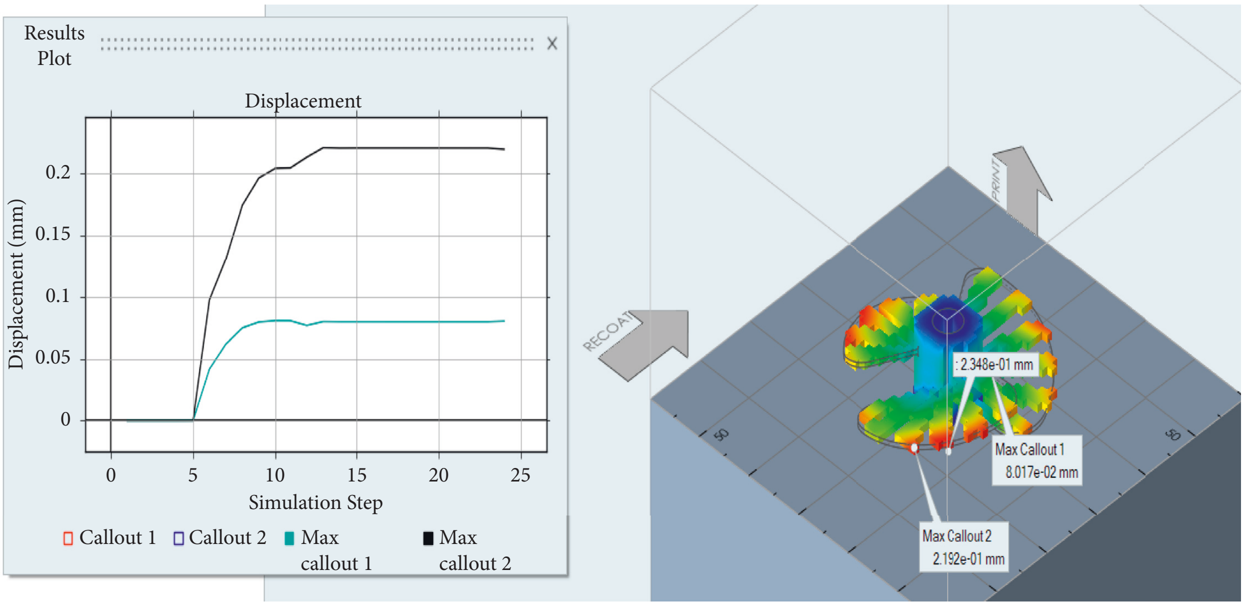

Figure 5: Displacement of various callout positions and a graph representing the displacement vs simulation step for Rank 10.

These positioning has been considered for our current study of the material behaviour and the positioning of the model will be as Figure 3.

6. Simulation

The simulation has been done in the Altair Inspire for undergoing thermomechanical analysis which helps us in studying the material behaviour along with the position of the part that has been chosen. The analysis went with the parameters resented in Table 6 with keeping the element or node size of length and height as 1 mm.

7. Results and Discussion

The simulation process has been completed without any errors and provided the details in Table 7 for the Rank 1 position. Figure 4 demonstrates the Von mises stress of various callout positions and the graph representing the von mises vs simulation step for Rank 1.

The simulation process has been completed without any errors and provided the details in Table 8 for the Rank 10 position. Figure 5 demonstrates the Von mises stress of various callout positions and the graph representing the von mises vs simulation step for Rank 10.

8. Conclusions

Out of all the results that have been captured with constant machine parameters. The displacement has very slight changes in the materials in comparison with the orientation of the part. The Plastic strain has very minimum effect throughout all the materials irrespective of the orientation of the part. The Von Mises Stress and the temperature is high in the SS 316L material in both the machines irrespective of the parameters. The minimum of maximum displacement 2.411e-01 mm was obtained in aluminium AlSi10 Mg in Rank 10 but in the case of the Rank 1, it was also as minimum as 2.348e-01 mm. In the same material, the minimum of maximum plastic strain was recorded in rank 10 and rank 1 are 0.1 and 0.05, respectively. In the case of Von mises stress, the minimum of maximum obtained for the Aluminium AlSi10 Mg materials are 6.655e+01 MPa and 2.086e+02 MPa for Rank 1 and Rank 10 respectively. Hence the Rank 1 and material of aluminium AlSi10 Mg was recommended for 3-blade Propeller.

Data Availability

The data used to support the findings of this study are included in the article. Should further data or information be required, these are available from the corresponding author upon request.

Conflicts of Interest

The authors declare that there are no conflicts of interest.

Acknowledgments

The authors would like to thank the Vels Institute of Science Technology and Advanced Studies, Chennai, for their excellent support for the submission of their papers. . It was performed as a part of the Employment Hawassa University, Ethiopia.

References

[1] S. L. Sing and S. Leong, "Perspectives on additive manufacturing enabled Beta- titanium alloys for biomedical applications," *International Journal of Bioprinting*, vol. 8, no. 1, p. 478, jan. 2022.

[2] W. Yu, Z. Xiao, X. Zhang et al., "Processing and characterization of crack-free 7075 aluminum alloys with elemental Zr modification by laser powder bed fusion," *Materials Science in Additive Manufacturing*, vol. 1, no. 1, p. 1, mar. 2022.

[3] S. Cacace and Q. Semeraro, "Fast optimisation procedure for the selection of L-PBF parameters based on utility function,"

Virtual and Physical Prototyping, vol. 17, no. 2, pp. 125–137, 2022.

[4] S. L. Sing, C. N. Kuo, C. T. Shih, C. C. Ho, and C. K. Chua, "Perspectives of using machine learning in laser powder bed fusion for metal additive manufacturing," *Virtual and Physical Prototyping*, vol. 16, no. 3, pp. 372–386, 2021.

[5] M. H. Sehhat, A. T. Sutton, C. H. Hung et al., "Plasma spheroidization of gas-atomized 304L stainless steel powder for laser powder bed fusion process," *Materials Science in Additive Manufacturing*, vol. 1, no. 1, p. 1, mar. 2022.

[6] X. Gong, D. Zeng, W. Groeneveld-Meijer, and G. Manogharan, "Additive manufacturing: a machine learning model of process-structure property linkages for machining behavior of Ti-6Al-4V," *Mater Sci Add Manuf*, vol. 1, no. 1, p. 6, 2022.

[7] A. Khobzi, F. Farhang Mehr, S. Cockcroft et al., "The role of block-type support structure design on the thermal field and deformation in components fabricated by laser powder bed fusion," *Additive Manufacturing*, vol. 51, Article ID 102644, 2022.

[8] K.-H. Lee and G. J. Yun, "Design Optimization of Thermally Conductive Support Structure for Laser Powder-Bed Fusion Process with Part-Scale thermal History," *Additive Manufacturing*, vol. 51, 2022.

[9] T. DebRoy, T. Mukherjee, J. O. Milewski et al., "Scientific, technological and economic issues in metal printing and their solutions," *Nature Materials*, vol. 18, no. 10, pp. 1026–1032, 2019.

[10] D. Herzog, V. Seyda, E. Wycisk, and C. Emmelmann, "Additive manufacturing of metals," *Acta Materialia*, vol. 117, pp. 371–392, 2016.

[11] S. Liu and Y. C. Shin, "Additive manufacturing of Ti6Al4V alloy: a review," *Materials & Design*, vol. 164, Article ID 107552, 2019.

[12] A. Fatemi, R. Molaei, J. Simsiriwong et al., "Fatigue behaviour of additive manufactured materials: an overview of some recent experimental studies onTi-6Al-4Vconsidering various processing and loading direction effects," *Fatigue and Fracture of Engineering Materials and Structures*, vol. 42, no. 5, pp. 991–1009, 2019.

[13] T. Kakiuchi, R. Kawaguchi, M. Nakajima, M. Hojo, K. Fujimoto, and Y. Uematsu, "Prediction of fatigue limit in additively manufactured Ti-6Al-4V alloy at elevated temperature," *International Journal of Fatigue*, vol. 126, pp. 55–61, 2019.

[14] S. Tammas-Williams, P. J. Withers, I. Todd, and P. B. Prangnell, "The influence of porosity on fatigue crack initiation in additively manufactured titanium components," *Scientific Reports*, vol. 7, no. 1, p. 7308, 2017.

[15] P. Edwards and M. Ramulu, "Fatigue performance evaluation of selective laser melted Ti-6Al-4V," *Materials Science and Engineering A*, vol. 598, pp. 327–337, 2014.

[16] Y. N. Hu, S. C. Wu, P. J. Withers et al., "The effect of manufacturing defects on the fatigue life of selective laser melted Ti-6Al-4V structures," *Materials & Design*, vol. 192, Article ID 108708, 2020.

[17] J. P. Oliveira, T. G. Santos, and R. M. Miranda, "Revisiting fundamental welding concepts to improve additive manufacturing: from theory to practice," *Progress in Materials Science*, vol. 107, Article ID 100590, 2020.

[18] S. C. Wu, C. Yu, P. S. Yu, J. Y. Buffière, L. Helfen, and Y. N. Fu, "Corner fatigue cracking behavior of hybrid laser AA7020 welds by synchrotron X-ray computed microtomography," *Materials Science and Engineering A*, vol. 651, pp. 604–614, 2016.

[19] M. Bayat, A. Thanki, S. Mohanty et al., "Keyhole-induced porosities in laser-based Powder Bed Fusion (L-PBF) of Ti6Al4V: high-fidelity modelling and experimental validation," *Additive Manufacturing*, vol. 30, Article ID 100835, 2019.

[20] Y. N. Hu, S. C. Wu, Z. K. Wu et al., "A new approach to correlate the defect population with the fatigue life of selective laser melted Ti-6Al-4V alloy," *International Journal of Fatigue*, vol. 136, Article ID 105584, 2020.

[21] R. Biswal, X. Zhang, M. Shamir et al., "Interrupted fatigue testing with periodic tomography to monitor porosity defects in wire + arc additive manufactured Ti-6Al-4V," *Additive Manufacturing*, vol. 28, pp. 517–527, 2019.

[22] D. Barba, C. Alabort, Y. T. Tang, M. J. Viscasillas, R. C. Reed, and E. Alabort, "On the size and orientation effect in additive manufactured Ti-6Al-4V," *Materials & Design*, vol. 186, Article ID 108235, 2020.

[23] S. Baskar, L. Karikalan, V. Vijayan, D. Arunkumar, and K. Sukenraj, "Performance, emission characteristics of compressed ignition engine with alternative fuel," *Materials Today Proceedings*, vol. 37, no. 2021, pp. 995–998, 2020.

[24] P. Ferro, A. Fabrizi, F. Berto, G. Savio, R. Meneghello, and S. Rosso, "Defects as a root cause of fatigue weakening of additively manufactured AlSi10Mg components," *Theoretical and Applied Fracture Mechanics*, vol. 108, Article ID 102611, 2020.

[25] M. Selvamuthukumar, B. Harish babu, S. bobba, S. Baskar, and N. Joy, "Investigation on the lubricating behavior of cashew nut shell liquid oil as a renewable and reliable petrochemical product," *Materials Today Proceedings*, vol. 44, no. 2021, pp. 3583–3588, 2020.

[26] S. Siddique, M. Imran, M. Rauer et al., "Computed tomography for characterization of fatigue performance of selective laser melted parts," *Materials & Design*, vol. 83, pp. 661–669, 2015.

[27] T. P. Chapman, K. M. Kareh, M. Knop et al., "Characterisation of short fatigue cracks in titanium alloy IMI 834 using X-ray microtomography," *Acta Materialia*, vol. 99, pp. 49–62, 2015.

[28] A. Du Plessis, I. Yadroitsava, S. G. Le Roux et al., "Prediction of mechanical performance of Ti6Al4V cast alloy based on microCT-based load simulation," *Journal of Alloys and Compounds*, vol. 724, pp. 267–274, 2017.

[29] L. Karikalan, S. Baskar, N. Poyyamozhi, and K. Negash, "Experimental analysis of heat transfer by using nanofluid and impact of thermophysical properties," *Journal of Nanomaterials*, vol. 2022, pp. 1–8, 2022.

[30] S. Khelge, V. Kumar, V. Shetty, and J. Kumaraswamy, "Effect of reinforcement particles on the mechanical and wear properties of aluminium alloy composites: Review," *Materials Today Proceedings*, vol. 52, no. 3, pp. 571–576, 2022.

[31] S. C. Wu, T. Q. Xiao, and P. J. Withers, "The imaging of failure in structural materials by synchrotron radiation X-ray microtomography," *Engineering Fracture Mechanics*, vol. 182, pp. 127–156, 2017.

[32] J. Kumaraswamy, V. Kumar, and G. Purushotham, "A review on mechanical and wear properties of ASTM a 494 M grade nickel-based alloy metal matrix composites," *Materials Today Proceedings*, vol. 37, pp. 2027–2032, 2021.

[33] K. Jayappa, V. Kumar, and G. G. Purushotham, "Effect of reinforcements on mechanical properties of nickel alloy hybrid metal matrix composites processed by sand mold technique," *Applied Science and Engineering Progress*, vol. 14, no. 1, pp. 44–51, 2020.

[34] M. I. Jordan and T. M. Mitchell, "Machine learning: trends, perspectives, and prospects," *Science*, vol. 349, no. 6245, pp. 255–260, 2015.